One Earth

Article

Restoring mangroves lost by aquaculture offers large blue carbon benefits

Graphical abstract

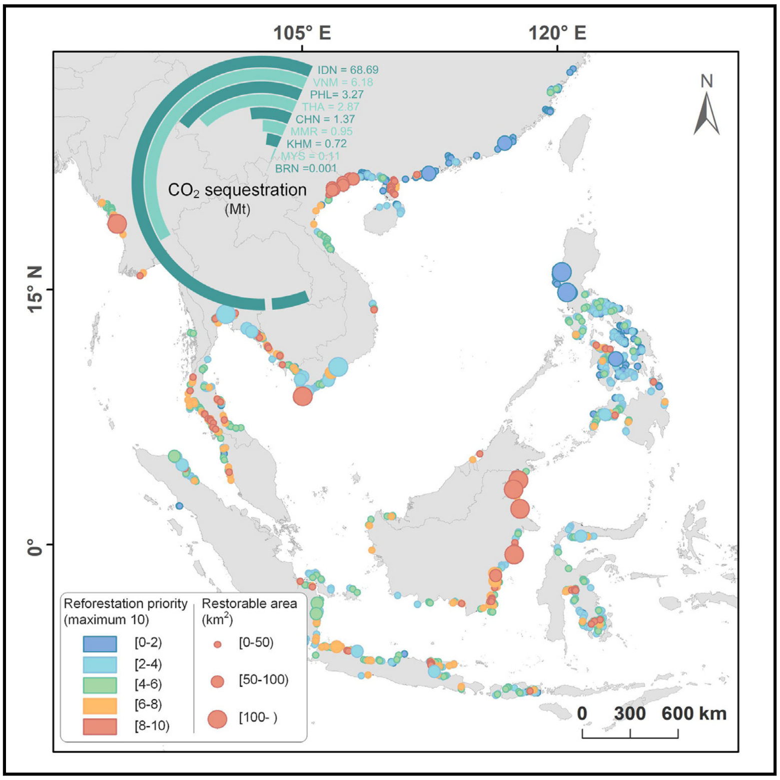

Highlights

- Aquaculture expansion in China and southeast Asia has caused substantial mangrove loss
- Approximately 60% of aquaculture ponds are suitable for mangrove restoration
- Indonesia is identified as a top priority for mangrove restoration efforts
- Priority restoration can remove 84 (75–96, 95% CI) Mt CO_2

Authors

Yufeng Jiang (姜玉峰), Zhen Zhang (张振), Daniel A. Friess, ..., Jing Li (李晶), Qian Zhang (张倩), Yi Li (李艺)

Correspondence

yangf@xmu.edu.cn (Y.L.),
yili@xmu.edu.cn (Y.L.)

In brief

Mangrove forests show great potential for mitigating climate change but have faced extensive deforestation due to aquaculture expansion. Aquaculture areas offer opportunities for mangrove restoration, as most still maintain suitable biophysical conditions. Here, we identify priority areas for mangrove restoration in China and southeast Asia. Priority restoration could remove 84 (75–96, 95% confidence interval) Mt CO_2. These findings can better formulate cost-effective strategies for mangrove restoration, thereby mitigating climate change more efficiently.

Jiang et al., 2025, One Earth *8*, 101149
January 17, 2025
https://doi.org/10.1016/j.oneear.2024.11.003

One Earth

CellPress

Article

Restoring mangroves lost by aquaculture offers large blue carbon benefits

Yufeng Jiang (姜玉峰),[1,3] Zhen Zhang (张振),[1,2,3] Daniel A. Friess,[2] Yangfan Li (李杨帆),[1,*] Zengkai Zhang (张增凯),[1] Ruirui Xin (信瑞瑞),[1] Jing Li (李晶),[1] Qian Zhang (张倩),[1] and Yi Li (李艺)[1,4,*]

[1]State Key Laboratory of Marine Environmental Science, Fujian Provincial Key Laboratory for Coastal Ecology and Environmental Studies, Key Laboratory of Coastal and Wetland Ecosystems (Ministry of Education), College of the Environment and Ecology, Xiamen University, Xiamen 361102, China

[2]Department of Earth and Environmental Sciences, Tulane University, New Orleans, LA 70118, USA

[3]These authors contributed equally

[4]Lead contact

*Correspondence: yangf@xmu.edu.cn (Y.L.), yili@xmu.edu.cn (Y.L.)

https://doi.org/10.1016/j.oneear.2024.11.003

SCIENCE FOR SOCIETY Conservation and restoration of blue carbon ecosystems, such as mangrove forests, represent a vital nature-based solution for climate change mitigation. Historically, mangroves have experienced extensive deforestation due to human activities, particularly aquaculture. Deforested areas now offer opportunities for achieving mangrove restoration targets, as they may still possess suitable environmental conditions for mangrove growth. Evaluating the feasibility of mangrove restoration at a fine scale allows for the identification of priority areas, thereby guiding on-the-ground restoration efforts. Our study indicates that aquaculture ponds historically converted from mangroves remain largely suitable for mangrove restoration and hold the potential for substantial blue carbon benefits. These findings can better formulate cost-effective strategies for mangrove restoration, thereby mitigating climate change more efficiently.

SUMMARY

Mangrove forests show great potential for mitigating climate change due to their high carbon densities but have faced extensive deforestation due to aquaculture. Aquaculture areas offer opportunities for mangrove restoration, as most still maintain suitable landscape-scale biophysical conditions. Despite this potential, the scale and biophysical suitability of aquaculture areas for large-scale mangrove restoration, along with associated carbon benefits and costs, remain poorly understood. We assess the restoration suitability of mangroves deforested by aquaculture and identify patch-scale priority areas in China and southeast Asia. Long-term satellite observations show that aquaculture expansion has caused the loss of 165,079 ha of mangroves. Habitat suitability modeling estimates that 60% of these lost mangroves are biophysically feasible for restoration and potentially removing 84 (75–96, 95% confidence interval) Mt CO_2. Our findings provide spatially explicit guidance for mangrove restoration planning and highlight the contribution that mangrove restoration can make to nationally determined contributions for climate change mitigation.

INTRODUCTION

Coastal wetlands, located at the land-sea interface, are vital ecosystems known for their rich biodiversity, high productivity, and the provision of a variety of ecosystem services.[1,2] Mangroves, in particular, are recognized as a promising natural climate solution (NCS) to offset greenhouse gas emissions and mitigate climate change.[3] Nevertheless, human activities in coastal regions have substantially reduced the global extent of mangroves, impacting their important ecological functions.[4,5] This widespread loss contributes to the annual release of 0.08–0.32 petagram (Pg) CO_2, accounting for ~2%–6% of the total CO_2 emissions from global deforestation.[6,7] Given their high carbon storage density over long timescales, the conservation and restoration of mangroves are an important NCS to draw down atmospheric carbon emissions for many countries.[8]

Through several international conservation strategies and policies, global mangrove restoration initiatives are collectively working to finance $4 billion USD to secure the future of over 15 million ha of mangroves globally by 2030.[9] Over the past 40 years, approximately 200,000 ha of mangroves have been planted, although the survival rates of planted mangroves are

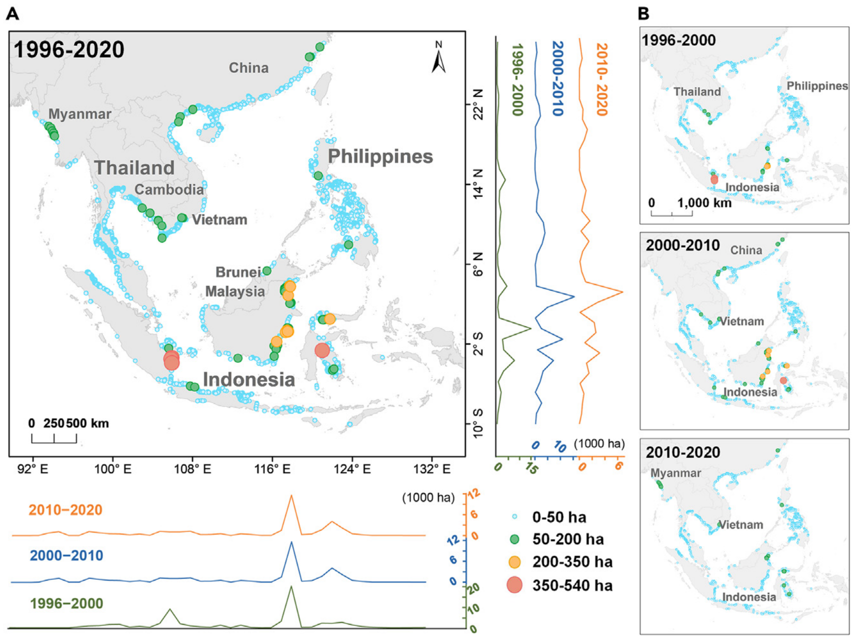

Figure 1. Spatial distribution of mangroves converted to aquaculture ponds in China and southeast Asia between 1996 and 2020

(A) Areas of mangrove loss due to aquaculture expansion between 1996 and 2020. The circle sizes represent the extent of lost mangrove areas. The colored lines depict the latitudinal trends of mangrove loss in different time periods (1996–2000, 2000–2010, and 2010–2020).

(B) The spatial distribution of lost mangrove areas for three periods (1996–2000, 2000–2010, and 2010–2020).

generally low.[10] For instance, Indonesia has planted around 24 million seedlings in 60 mangrove restoration projects, but many of these initiatives have failed.[11,12] Low survival rates are primarily due to afforestation and restoration efforts being conducted in areas biophysically unsuitable for mangrove growth.[13,14] Recent studies indicate that successful mangrove restoration yields greater carbon benefits compared to afforestation,[15] suggesting that management initiatives should prioritize restoration—for example, planting in historically existing mangrove areas. Consequently, stakeholders have advocated for a shift in mangrove restoration targets from simply expanding planted areas to improving the success of large-scale restoration by identifying feasible biophysical locations for restoration.[12,16]

The expansion of aquaculture ponds has been the primary anthropogenic factor causing mangrove loss over the past few decades,[17] especially in China and southeast Asia[18,19] (including Brunei, Cambodia, Indonesia, Myanmar, Malaysia, the Philippines, Singapore, Thailand, Timor-Leste, and Vietnam). The development of aquaculture ponds has led to widespread mangrove deforestation, yet these areas often still possess macroclimatic, environmental, and hydrodynamic conditions favorable for mangrove growth,[20] and thus provide potential priority settings for mangrove restoration.[21] Prior research has assessed suitable areas for mangrove restoration globally,[10] or for a specific country,[12] although they primarily offer a broad perspective on which broad landscapes deserve more attention for mangrove restoration, lacking detailed patch-scale information that focuses specifically on the restoration of aquaculture ponds, the main driver of mangrove loss. As a result, spatially explicit quantitative estimates of the carbon and economic benefits associated with mangrove restoration are highly anticipated.

Here, we (1) map the spatial distribution of mangrove deforestation driven by aquaculture expansion and quantify the associated carbon emissions, and (2) identify priority areas within aquaculture ponds for potential mangrove restoration, factoring in restoration costs and carbon benefits. We first mapped mangrove loss attributed to aquaculture by cross-referencing mangrove and aquaculture cover data in China and southeast Asia, where >32% of the global mangrove extent is located[22] and has experienced substantial aquaculture expansion since the 1970s.[23] We then applied a habitat suitability model to determine aquaculture ponds that should be prioritized for mangrove restoration, considering eight biophysical factors related to mangrove establishment and growth attributes, such as climate, marine environment, and human disturbance. We further estimated carbon losses from mangrove deforestation due to aquaculture and assessed the potential carbon and economic benefits of mangrove restoration in these priority areas. Our findings indicate that aquaculture ponds contributed to approximately 25% of mangrove deforestation in China and southeast Asia since 1996, with >60% of these ponds retaining favorable conditions for restoration, potentially offsetting 3% of carbon emissions from deforestation in these regions. Our study highlights the cost-effectiveness and carbon advantages of restoring mangrove forests within their historical ranges, offering actionable insights for policymakers and stakeholders to support forest restoration and carbon mitigation objectives.

RESULTS AND DISCUSSION

Aquaculture-induced mangrove loss, 1996–2020

Using object-oriented image classification techniques, we mapped mangrove patches deforested due to aquaculture expansion and detected widespread mangrove deforestation across China and southeast Asia from 1996 to 2020 (Figure 1). The mangrove area decreased by 165,079.38 ha, which corresponds to a 25% reduction of the mangrove area in China and southeast Asia since 1996. Indonesia experienced the largest aquaculture-induced mangrove losses—118,781.13 ha—accounting for 72.0% of total mangrove losses caused by aquaculture ponds in the study region (Figures 2, S1, and S2), followed by Vietnam and the Philippines, with 19,392.50 ha (11.7% of total) and 9,670.36 ha (5.9% of total), respectively. Compared to a previous study,[19] our results identified more deforested mangrove areas due to aquaculture, particularly in Indonesia and Vietnam (Table S1). This discrepancy is primarily due to differences in methodology and data sources used for mapping aquaculture

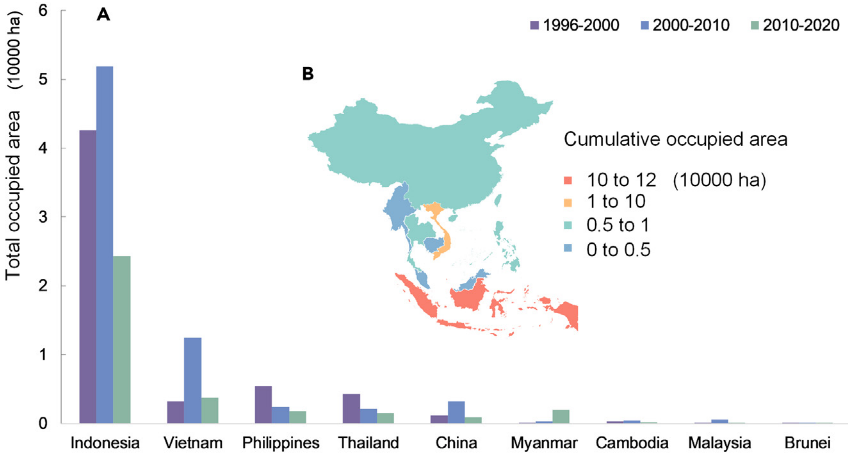

Figure 2. Area of mangroves converted to aquaculture ponds in 1996–2020, by country

(A) The total area of mangroves converted to aquaculture ponds at different periods provided by countries. Datasets in Singapore and Timor-Leste are not shown in the bar chart due to no detected mangrove patches converted to aquaculture ponds in these two countries over the period of this study.

(B) Cumulative aquaculture-induced mangrove loss areas between 1996 and 2020 illustrated with spatial distribution maps.

ponds and mangrove deforestation. In 2016, Richards and Friess[19] adapted a global deforestation model not specifically designed for mangrove forests and excluded deforested mangrove patches smaller than 0.5 ha (i.e., 5–6 Landsat pixels), which likely led to an underestimation of mangrove loss caused by the development of small aquaculture ponds. In contrast, our estimate is based on a mangrove-specific change map combined with an advanced aquaculture pond data product, allowing us to more accurately detect mangrove deforestation due to aquaculture.

The rate of mangrove loss due to aquaculture ponds declined in most countries between 2010 and 2020. The highest loss occurred between 2000 and 2010, primarily in Indonesia and Vietnam. In contrast, the Philippines and Thailand showed a continuous downward trend in mangrove loss (Figure 2A) across the 1996–2020 period. The declining rate of mangrove loss illustrates the effectiveness of existing conservation efforts in preventing further mangrove deforestation in China and southeast Asia,[24,25] alongside changes in industrial approaches to aquaculture, which has shifted from area expansion to increasing productivity.[26] Our spatially explicit results are consistent with the observed changes in the aquaculture industry in southeast Asia, where government policies have curbed deforestation for pond construction driven by economic demand, leading to a gradual slowdown in expansion. With economic development policies, coastal aquaculture ponds evolved into an export-oriented commercial mode,[26] leading to rapid expansion and increased density of agricultural activities.[27] This trend was particularly evident in Indonesia until the designation of mangroves as protected forests under Law 5/1990 and Presidential Decree 32/1990,[12,28] coupled with the impact of the economic crisis, which led to a decline in the rate of mangrove loss.

Biophysically feasible areas for mangrove restoration

We evaluated the suitability of restoration for each aquaculture pond patch converted from mangroves before 2020, using the habitat assessment model MaxEnt, considering eight important biophysical factors affecting mangrove survival and growth. We normalized the suitability results and divided them into five categories based on suitability scores, with higher scores indicating higher priority for restoration. We found that approximately 76,399 ha (∼60%) of aquaculture ponds demonstrated high priority for mangrove restoration (Figures 3 and S3), contributing to approximately 12% of global highly restorable mangrove targets in terms of area.[29] The regions with the highest biophysical feasibility for restoration were concentrated along the east coast of Samarinda (117.48°E, 0.59°S) and Tarakan (117.75°E, 3.76°N) in Indonesia, as well as in Ngoc Hien (105.01°E, 8.69°N) in southern Vietnam. Notably, Indonesia stands out as the country with the greatest potential for mangrove restoration, comprising 86% of the identified biophysically feasible areas within the study region (Figures S4 and S5). Our results align with assessments from the Global Mangrove Alliance and recent studies,[12] underscoring the substantial opportunities for future restoration arising from the historical rates of mangrove loss in Indonesia due to aquaculture.

We then categorized aquaculture-induced mangrove losses into three distinct time periods (1996–2000, 2000–2010, and 2010–2020) and calculated the average restoration feasibility of each period. It was observed that the deforested mangrove patches from 2000 to 2010 exhibited the highest biophysical feasibility for restoration, probably due to the relatively lower magnitude of mangrove fragmentation during this specific period compared to other periods (Figure S6; Table S2).

To establish clear environmental benchmarks for the construction of mangrove restoration projects, we further extracted the range of eight biophysical indicators for the identified high-priority mangrove restoration areas (Table S3). We found that areas characterized by continuous mangrove patches (6.6–79.3 patch per hectare, 95% confidence interval [CI]), high tidal ranges (1.4–3.2 m), and low rates of sea-level rise (1.2–5.1 mm/year) are particularly suitable for mangrove restoration (Table S4). Regions characterized by continuous mangrove patches represent low fragmentation, thus holding more core habitats to resist external disturbances.[30] Ecosystems with less fragmentation could create a more favorable habitat for the survival of mangrove seedlings, leading to exceptional restoration outcomes and improved efficiency.[31] Various benthic organisms within the mangrove ecosystem contribute to the decomposition of organic matter in the soil,[32] providing comprehensive nutrition for the growth of mangrove seedlings,[33] and thereby enhancing the efficiency of restoration. Successful mangrove restoration also relies on favorable hydrological conditions, including adequate periods free from tidal inundation, sufficient freshwater supply, and moderate wave action.[34–36] Mangrove seedlings are highly sensitive to the depth and duration of tidal inundation. Prolonged periods of flooding can hinder and impede the growth and survival of mangroves.[37,38]

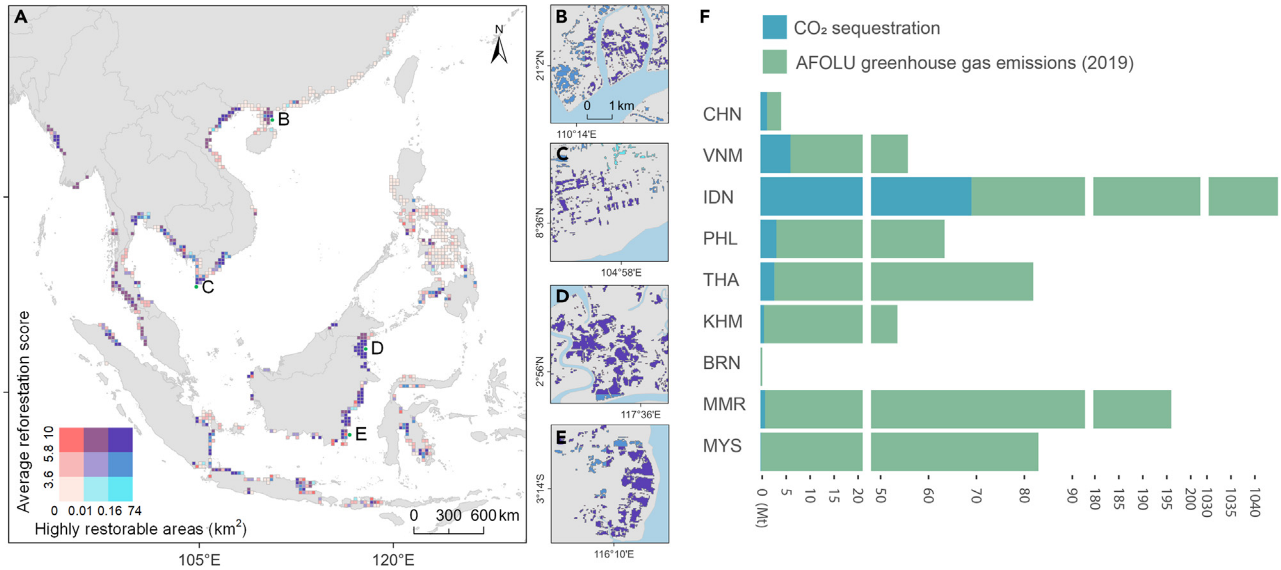

Figure 3. Distribution of biophysical feasibility of mangrove restoration across China and southeast Asia

(A) The nine colors show biophysical feasibility of the restorable area within 0.25° cells. The raster grid maps for the bivariate variables are presented from average restoration score and highly restorable areas perspectives. Biophysical feasibility of the restorable area was given in nine colors according to the ranking of feasibility values and highly restorable areas. Areas in red represent the location with highest feasibility, and brilliant blue represents the most area of highly restorable.

(B–E) The map also shows the locations of the highly restorable field sites.

(F) Estimated CO_2 sequestration from mangrove restoration in relation to the 2019 AFOLU greenhouse gas emissions (note log scale). The CO_2 sequestration potential of restorable mangroves (including biophysically feasible restoration of occupied mangroves in study region over the next 40 years) gained from above-ground biomass, below-ground biomass, and soil organic carbon to 1-m depths. Datasets in Singapore and Timor-Leste are not shown in the bar chart due to no detected area of biophysical feasibility of mangrove restoration in these two countries. BRN, Brunei; CHN, China; IDN, Indonesia; KHM, Cambodia; MMR, Myanmar; MYS, Malaysia; PHL, Philippines; THA, Thailand; VNM, Vietnam.

Moreover, mangroves in environments with high tidal ranges have greater elevation capital than those in lower tidal ranges, so they are considered less vulnerable to sea-level rise.[39] Additionally, salinity (Table S4) is an important additional environmental factor for successful mangrove restoration.

Carbon benefits of mangrove restoration

Mangrove deforestation releases substantial amounts of carbon into the atmosphere, but restoration efforts can help draw down atmospheric carbon. Based on changes in mangrove area and spatial carbon data (see experimental procedures for details), we estimate that the expansion of aquaculture ponds in China and southeast Asia from 1996 to 2020 has resulted in the loss of 20 (11–29, 95% CI) Mt of biomass carbon and 32 (20–45) Mt of soil organic carbon (SOC; to a depth of 1 m). Combined, these losses account for a total carbon emission of 192 (114–270, 95% CI) Mt CO_2 (Table S5), equivalent to 0.5% of the greenhouse gas emissions from agriculture, forestry, and other land use (AFOLU) sectors in the region during the same period.[40] These carbon losses equate to an economic value loss of approximately $1,881 (427–2,560, standard errors) million USD, based on the social cost of carbon.[41] Indonesia, having experienced the highest amount of mangrove loss and possessing mangroves with high carbon density, alone accounts for $1,650 (382–2,218, standard errors) million USD of this total loss.

Considering that the cost of mangrove restoration may vary between countries,[42,43] we determined the restoration cost based on the historical literature (see experimental procedures for details), revealing an approximate cost of $6,063 ($2,163–$9,963) USD ha^{-1} (mean, 95% CI), with a median value of $1,359 USD ha^{-1} and a range of minimum to maximum values from 155 to $76,062 USD ha^{-1}. By referencing the blue carbon price traded through the global carbon exchange Climate Impact X (CIX) and the carbon finance business Respira,[44] the restoration of identified priority areas may cost $463 (95% CI 165–761) million USD in total, but could result in carbon credit benefits worth $638 (95% CI 567–725) million USD over the next 40 years, with 84 (75–96) Mt CO_2 in total (Figure 3F). Among these countries, Indonesia receives the highest carbon benefits from mangroves, removing approximately 69 (61–79) Mt CO_2 (Figures 3F and S5). We compared our result (Table S6) with the carbon benefits of mangrove restoration reported by previous studies. The estimation of the sum of restorable carbon by Worthington et al.[10] is approximately seven times greater than our results, primarily due to their assessment of a restoration area four times larger than ours. Our study focuses specifically on restoration targets limited to mangrove areas lost due to aquaculture expansion. Additionally, we took into account the non-linear growth of carbon accumulation in the early stages of mangrove growth, along with factors such as allochthonous carbon removal (as required by leading carbon credit verification methodologies), all contributing to our lower sum of carbon restorables compared to Worthington et al.[10] Our calculated average density of total carbon for restorable areas in each country is lower than that from Worthington et al. by approximately 82 Mg C/ha. In terms of average carbon density, the difference is minimal, with the exception of the Philippines. The variation with the Philippines is mainly attributable to a large contribution from biomass carbon. Our sum of restorable carbon in Indonesia is three times greater than that estimated by Sasmito et al.[12] due to the fact that they estimated carbon sequestration for the years 2021–2025, while we estimated it for a period of 40 years. Additionally, they excluded dead wood and soil carbon stocks in their assessment of carbon storage. Our longer evaluation period and inclusion of a more comprehensive carbon storage inventory results in a larger sum of carbon restorable compared to their estimation. Practically speaking, the contributions of mangrove restoration projects to human society are even higher than the assessed carbon market value due to other ecosystem services such as fisheries production and coastal protection.[45] Implementing biophysically feasible restoration in aquaculture areas would result in extra 32 (28–36) Mt CO_2 removal than afforesting in areas where mangroves have not grown, which is equal to \$239 (95% CI 212–272) million USD.[15]

Numerous countries within the study region have proactively embraced national climate policies in alignment with the climate change mitigation objectives outlined in their nationally determined contributions (NDCs) to the Paris Agreement. The identified opportunities for mangrove restoration could make a meaningful contribution to the NDCs of certain countries. Based on the datasets from the Net Zero Tracker, Climate Action Tracker public policy database, and carbon emissions data from the World Bank, we compiled the climate change efforts of these countries (Figure S7). In general, the implementation of feasible mangrove restoration in China and southeast Asia can annually offset approximately 0.2% of 2019 AFOLU greenhouse gas emissions (Figure 3F). This is equivalent to the CO_2 emissions of approximately 18 (16–21) million people in Asia for the year 2022, aiding emission reduction efforts and contributing to climate improvement (Sustainable Development Goal 13).

Given the potential carbon benefits of mangroves, several countries in the region are advancing plans for mangrove conservation and restoration. The Indonesian government has explicitly incorporated mangrove restoration as a component of its latest submitted NDC, aiming to greatly contribute to the country's self-determined initiatives. Specifically, the government of Indonesia has set an ambitious target of 600,000 ha of mangrove restoration by 2024.[46] Implementing blue carbon strategies can address climate change through nature-based solutions and promote economic synergy between various sectors on land and in the ocean.[8] Net-zero emissions are a common but differentiated responsibility for national governments. Governments should encourage businesses and organizations, together with individuals, to increase financing for mangrove restoration projects in the study region,[47] to achieve the goal of securing the future of over 15 million ha of mangroves globally by 2030, underpinned by \$4,000 million USD of sustainable finance.

It should be noted that while our results provide spatially explicit high-priority areas for guiding mangrove restoration based on landscape scale biophysical parameters, the implementation of restoration on the ground will be determined by a range of socioeconomic factors such as land tenure arrangements, the willingness of pond owners to restore, the opportunity costs of restored land, as well as local-scale biophysical conditions such as tidal inundation and microtopography.[36,48,49] These socioeconomic and biophysical factors vary greatly over small scales, so they cannot be mapped at the continental scale. Future research could focus on identifying abandoned aquaculture ponds to cut down restoration costs, as well as utilizing more detailed data to better characterize local factors. These considerations can further optimize the identification of the most biophysically feasible areas for mangrove restoration in terms of success rate and cost-effectiveness. Additionally, considering other greenhouse gas emissions such as methane emissions from mangroves and CO_2 release from $CaCO_3$ formation could improve the carbon accounting of mangrove deforestation and restoration.

In summary, through the development of aquaculture-mangrove change maps and consideration of biophysical factors (e.g., tidal range, sea surface temperature), this study identified spatial-explicit opportunities for mangrove restoration to guide decision-makers to achieve national-level climate mitigation goals in China and southeast Asia. Restoring mangroves in these identified locations can provide important blue carbon benefits, equivalent to offsetting 3% of China and southeast Asia's carbon emissions caused by deforestation,[40] emphasizing the great potential of mangrove blue carbon restoration as an important NCS. Biophysically feasible restoration of mangroves also results in a net benefit of \$175 (95% CI −194 to 560) million USD. The spatial feasibility map can demonstrate government opportunities for strategic action to support and advance successful blue carbon projects. Restoring, conserving, and managing mangroves in places with suitable environmental conditions represent a cost-effective option to improve the capacity of capturing and storing carbon contributing to global goals.

EXPERIMENTAL PROCEDURES

Study region

Southeast Asia is recognized a global hotspot for mangrove distribution, holding nearly one-third of the world's mangrove forests, with diverse tree species and substantial carbon storage.[50,51] However, the region has also experienced extensive mangrove losses.[4,52] In addition to southeast Asia, China has suffered considerable mangrove loss in recent decades, largely attributed to coastal aquaculture development.[53] Consequently, we included China in our analysis to ensure comprehensive coverage of mangroves and coastal aquaculture ponds. To achieve this, our analysis was confined to Landsat scenes that intersected with the 30-km buffer of the coastline (the mean scene size is $\sim$170 × 183 km).[54] Considering both mangroves and coastal aquaculture ponds are distributed in flat and open tidal flats, we retained areas of coastal plains with an elevation <10 m[54] as potential areas for mapping coastal land-based aquaculture ponds in China and southeast Asia using the SRTM V3 DEM dataset.[55]

Mapping coastal aquaculture ponds

We analyzed 80,694 archived images from Landsat 5, 7, and 8 with Google Earth Engine to create a distribution map of aquaculture ponds in China and southeast Asia. The Landsat data from three periods (1999–2001, 2009–2011, and 2019–2021) underwent pre-processing to ensure accurate surface reflectance measurements. Pixels with cloud cover and shadows were excluded from the image stack using the CFmask algorithm to maintain data integrity.[56,57] For classification, we developed a tailored training and validation dataset for the study region (Note S1), comprising 6,714 accurately labeled locations of coastal aquaculture ponds and non-aquaculture ponds (e.g., salt pans, offshore waters, rivers, lakes, irrigation channels).

We first extracted water bodies within the coastal buffer zone and excluded the interference of temporarily inundated areas. We then applied object-oriented K-nearest neighbor (KNN) classification to the long-term inundated areas to obtain an accurate map of coastal aquaculture ponds. Specifically, we used the widely applied modified normalized difference water index to extract water bodies. The Otsu thresholding[58] method provided automated efficiency for this extraction process. The water body pixel results derived from a single snapshot included both long-term inundated aquaculture ponds and temporarily inundated areas such as salt pans. To eliminate the interference of temporarily inundated waters, we created a water inundation frequency feature based on long-term satellite imagery.[59] By analyzing two training datasets, we determined that the inundation frequency threshold for identifying aquaculture ponds was >25% (Figure S8). After multi-level rule filtering, the remaining water bodies were identified as long-term inundated areas. Nevertheless, it is important to note that natural water bodies (e.g., rivers, lakes) may still exist within the long-term inundation area results. The most significant spatial difference between aquaculture ponds and natural water bodies is their shape, as ponds typically exhibit regular shapes like rectangles or squares. Therefore, we employed an object-oriented classification method with multi-scale segmentation to effectively differentiate aquaculture ponds and natural water bodies.[18] We established spectral, geometric, texture, and water inundation frequency features for the subsequent classification process (Table S7). Through feature space optimization, we targeted the best set of features to effectively differentiate aquaculture and non-aquaculture ponds in long-term inundated water bodies. Finally, the accurate extraction of coastal aquaculture ponds was achieved using the KNN classification method based on a random 70% of the sample points from the dataset based on the distribution in study region.

Through validation using 6,714 samples, we found that our aquaculture pond data achieves an overall accuracy exceeding 90%, with producer's accuracy and user's accuracy at 97% and 86%, respectively (Table S8; Note S1). In 2020, the aquaculture ponds map had a high overall accuracy of 92.7% and an F1 score of 0.94. Compared to previous aquaculture pond mapping studies, our data product effectively excludes water bodies having similar characteristics with aquaculture ponds, such as salt ponds and rice paddies, by combining water frequency thresholds and spectral signature (Figures S8–S11; Note S2).

Determining mangrove loss areas caused by aquaculture ponds

To determine areas where mangroves have been occupied by aquaculture ponds in China and southeast Asia since 1996, we conducted an overlay analysis of early-period mangrove datasets with later-period aquaculture pond datasets. The primary mangrove datasets used in this study were sourced from Global Mangrove Watch (GMW),[60] supplemented by additional datasets[61,62] to rectify any inaccuracies within the GMW datasets. To minimize errors, we proportionally removed mangrove pixels with low NDVI (normalized difference vegetation index) rankings based on the reported errors rates in these datasets and removed a corresponding proportion of high-ranked NDVI pixels from the aquaculture pond results based on the validation accuracy. This was done to mitigate the mixing of image pixels and reduce the impact of the interference caused by the surrounding mangroves' growth around aquaculture ponds. The GMW mangrove dataset served as the primary source, bolstered by error removal and effective supplementation from other datasets.[61,62] Subsequently, we removed the mangrove data from the aquaculture pond data to ensure their independence. After separately processing the datasets to account for errors in both mangroves and aquaculture ponds as mentioned above, we spatially overlaid the two datasets to identify areas where land use-type transitions occurred. The mangrove datasets representing areas occupied by aquaculture ponds were collected for three periods: 1996–2000, 2000–2010, and 2010–2020. Due to the limited presence of aquaculture ponds and mangroves detected in both Singapore and Timor-Leste and the absence of spatially overlapping areas, no instances of mangrove occupied by aquaculture ponds during the time period coverage of the GMW dataset were detected in these two countries.

Calculating biophysical feasibility for restoration areas

Historical mangrove areas provide favorable settings for mangrove restoration due to suitable environmental factors.[61] As a major driving factor of mangrove loss in China and southeast Asia, the aquaculture ponds gained from historic mangrove patches offer a potential opportunity for mangrove restoration. The estimation period was between 1996 and 2020, during which we identified areas that were originally mangroves but had been converted to aquaculture ponds. These areas remained aquaculture ponds up until 2020. Adequate tidal range, hydrological conditions, and the rate of sea-level rise have been identified as crucial factors for mangrove growth.[34,63,64] Additionally, environments characterized by high biodiversity, low salinity, humid climate, and minimal human disturbance are beneficial for mangrove rehabilitation.[43,65–67] Therefore, we included eight ecological and socio-environmental indicators in habitat suitability assessment, including mangrove patch density (the number of mangrove patches per hectare), rate of sea-level rise, tidal range, sea surface salinity,[68] precipitation, sea surface temperature, air temperature, and human disturbance (detailed parameters and acquisition methods are provided in Table S4). In regions where coastal data were incomplete, we employed spatially focused statistical methods to supplement the data.

To conduct the species suitability assessment, we developed a training dataset representing the distribution in study region, consisting of 452 accurately located samples of aquaculture ponds that have successfully been restored to mangroves and samples of land that have remained mangrove habitat. Using the MaxEnt model based on the maximum entropy theory,[69] we identified potential habitats suitable for mangrove restoration. MaxEnt is a statistical methodology employed to infer the relationship between species records within specific locations and the corresponding environmental and/or spatial attributes of those sites.[70] The approach has the advantage of being more robust and high performing than other species niche models. We used environmental variables to identify key factors limiting mangrove growth and distribution by finding the closest geographic uniform and the least constrained species distribution.[69,71] To ensure the independence of environmental variables, only those variable pairs with Pearson correlation coefficients lower than 0.8 were used in the MaxEnt model (Table S4). Ultimately, we normalized the values of suitable habitats to obtain a mangrove survival suitability score map with spatial locations. Based on a prioritization scale ranging from 0 to 1, the restorable regions were divided into five equal levels on average, with higher scores indicating higher restoration priority. We defined the two highest-level regions as biophysically feasible areas suitable for mangrove restoration.

We documented the time of land use conversion in these regions and, after obtaining the results for restoration feasibility, conducted statistical analyses on different time periods and their respective areas. Additionally, statistical analysis was performed on the value ranges of eight environmental factors in the top two biophysically feasible groups, excluding outliers. This value range was defined as the suitable environmental parameters for mangrove growth.

Estimating costs and benefits of mangrove loss and restoration

Mangrove carbon stock consists of above-ground biomass (AGB), below-ground biomass (BGB), and SOC.[72,73] AGB was calculated for each mangrove patch according to an empirical model proposed by previous research[74,75]:

$$AGB_i = (-4.617 \times |lat| + 239.9) \times Area_i \times 0.0001, \quad \text{(Equation 1)}$$

where $|lat|$ is the absolute latitude and $Area_i$ is the area of mangrove patch_i in square meters.

BGB was computed from allometric methods based on the ratio of mangrove AGB at the patch scale. Considering spatial variations between regions, we used the mid-value of 0.5 from the AGB to BGB ratio range of 0.39–0.61 provided by existing studies for our estimations.[76–79] We then chose a conversion factor of 0.451,[40,80] within the range of 0.45–0.50,[6,72] to estimate mangrove carbon storage from whole-tree mangrove biomass, as recommended by the Intergovernmental Panel on Climate Change (IPCC) guidelines. The calculation of total soil carbon stocks to 1-m depths is based on the average carbon density[50,81] within a 1° grid and the area of mangroves before deforestation.

AGB, BGB, and SOC constitute the carbon emissions resulting from mangrove loss, calculated as follows:

$$CO_2 \text{ emissions} = [\beta 1 * (AGB + BGB) + \beta 2 * SOC] \times 3.67, \quad \text{(Equation 2)}$$

where $\beta 1$ and $\beta 2$ are the emission factors for biomass and SOC due to mangrove deforestation, determined to be 83% (95% CI 46%–120%) and 52% (95% CI 32%–72%),[82,83] respectively, based on existing studies. The calculated carbon emissions were then converted to CO_2 emissions by multiplying by a coefficient of 3.67,[84] which is the molecular weight ratio of CO_2 to carbon.

The carbon benefits of mangrove restoration are also calculated from both biomass and SOC, typically stabilizing about 40 years, according to a recent study.[85] Biomass calculations follow the method outlined in Equation 1, but the carbon stock in restored mangrove biomass culminated at 72% to that of intact stands.[86] The SOC gain depends on the number of years and the annual carbon burial rate, which is set as 2.60 (95% CI 2.08–3.12) Mg C ha^{-1} $year^{-1}$ based on the average values compiled from Breithaupt and Steinmuller[87] for China and southeast Asia. This value is higher than the global average mangrove carbon burial rate provided by the Verified Carbon Standard VM0033 Methodology for Tidal Wetland and Seagrass Restoration (1.46 mg C ha^{-1} $year^{-1}$) and the IPCC (1.62 mg C ha^{-1} $year^{-1}$) but is considered reasonable given that mangroves in southeast Asia have higher-than-average carbon density, canopy height, and biomass.[88] Considering that the soil carbon burial rate is lower during the initial 5 years of mangrove canopy development (when the canopy cover is less than 50%),[85] we performed a non-linear interpolation to estimate the annual carbon burial rate for the first 5 years[86] (Equation 3). Additionally, we excluded the average proportions of allochthonous carbon from SOC calculations, which constitutes approximately 24%–55% of SOC in Vietnam,[89] 3%–73% in China,[90] and 13%–47% in Indonesia.[91] For countries where allochthonous carbon data are not available, we used values from nearby countries with available data.

$$Rate_t = 1.62 * \ln(year_t), \quad \text{(Equation 3)}$$

$$SOC_{SUM} = (1 - \%C_{alloch})\left\{\left(\sum_{year=1}^{5} Rate_t * Area * year_t\right) + (Rate_{soc35} * Area * 35)\right\}, \quad \text{(Equation 4)}$$

$$C_{SUM} = SOC_{SUM} + C_{biomass}, \quad \text{(Equation 5)}$$

where $Rate_t$ is the soil carbon accumulation rate for the year t in the first 5 years, $Rate_{SOC35}$ is the soil carbon accumulation rates from 5 to 40 years, SOC_{SUM} is the total of soil carbon accumulation for 40 years, $\%C_{alloch}$ is the proportion of allochthonous carbon, C_{SUM} is the cumulative total carbon benefit, and $C_{biomass}$ is the biomass carbon.

To comprehensively evaluate the status of mangrove forests, the costs associated with mangrove restoration vs. the carbon benefits derived from it are the crucial factors.[43] We used the country-level social cost of carbon (CSCC) to measure the expected economic loss from CO_2 emissions.[92–95] By combining socio-economic, climate, and impact data, we extracted the CSCC for study region based on a specific case assessment. To estimate the CSCC, we considered the socio-economic scenario (SSP2) and related climate scenario (RCP6.0), with the central specification of the Burke-Hsiang-Miguel damage function (short run, no income differentiation) and a growth-adjusted discount rate ($\rho = 2\%$, $\mu = 1.5$).[41] In assessing the restoration costs for mangrove restoration projects in study regions, we considered inflation and extreme errors, referring to the method from Bayraktarov et al.[42] and Su et al.[43] The costs of mangrove restoration projects in China and southeast Asia encompass several key categories: capital costs (including planning, land acquisition, financing, and purchasing), engineering costs (pit digging, planting, and construction), operating costs (maintenance, monitoring, transportation, and equipment repair and replacement), and in-kind costs (donations or volunteer labor). The values of mangrove restoration cost vary in every country, depending on maintenance and labor costs, making it challenging to determine a precise value. As such, we reported the restoration costs based on the minimum, median, mean (95% CI), and maximum to provide a cost uncertainty range. Furthermore, the opportunity cost of restoring aquaculture ponds into mangroves, as well as the wider cumulative effects of mangrove restoration actions, such as impacts on global aquatic product supply and deforestation transfer to other continents, are not included in our accounting due to the huge uncertainties. We look at overall carbon credit generation but do not estimate long-term opportunity costs. Not incorporating these factors into our cost analysis could result in the actual costs being more than an order of magnitude higher than the average value. Based on the blue carbon prices traded through CIX and the carbon finance business Respira, it was assumed that the implementation of mangrove restoration would generate a revenue of $27.8 USD/tonne.[96]

RESOURCE AVAILABILITY

Lead contact

Further information and requests for datasets should be directed to the lead contact, Yi Li (yili@xmu.edu.cn).

Materials availability

This study did not generate new unique materials.

Data and code availability

All data used in this study are publicly available online. The distribution of biophysical feasibility of mangrove restoration data products are viewable at Google Earth Engine (https://ee-zq970919.projects.earthengine.app/view/mangrove-reforestation-priority, last access: November 21, 2024), and are publicly available as of the date of publication at Zenodo (https://zenodo.org/records/11206627, last access: November 21, 2024). The Landsat 30-m spectral reflectance data (Landsat 5 Surface Reflectance, Landsat 7 Surface Reflectance, and Landsat 8 Surface Reflectance) are available at Google Earth Engine (https://developers.google.com/earthengine/datasets/catalog/LANDSAT_LT05_C01_T1_SR, https://developers.google.com/earthengine/datasets/catalog/LANDSAT_LE07_C01_T1_SR, and https://developers.google.com/earthengine/datasets/catalog/LANDSAT_LC08_C01_T1_SR, last access: November 21, 2024). Coastline data can be accessed at OpenStreetMap (https://www.openstreetmap.org, last access: November 21, 2024). Digital elevation model data are provided by NASA JPL at a resolution of 1 arc-second and is available at Google Earth Engine (https://developers.google.com/earth-engine/datasets/catalog/USGS_SRTMGL1_003, last access: November 21, 2024). Mangrove forests cover data are provided by Global Mangrove Watch at a resolution of 30 m and can be accessed on Zenodo (https://zenodo.org/record/6894273, last access: November 21, 2024). Global mangrove forests distribution, v1 (2000) are provided by NASA SEDAC at Google Earth Engine (https://developers.google.com/earth-engine/datasets/catalog/LANDSAT_MANGROVE_FORESTS, last access: November 21, 2024). And other mangrove forests cover data (ESA WorldCover 10m v100) are provided by ESA at Google Earth Engine (https://developers.google.com/earth-engine/datasets/catalog/ESA_WorldCover_v100, last access: November 21, 2024). Coastal aquaculture ponds cover data in this study have been deposited at Zenodo (https://doi.org/10.5281/zenodo.8344132, last access: November 21, 2024). Climate data used in this study are from WorldClim (https://www.worldclim.org/data/index.html, last access: November 21, 2024). Sea-level rise data are provided by National Oceanic and Atmospheric Administrationare (https://tidesandcurrents.noaa.gov/sltrends/mslGlobalTrendsTable.html, last access: November 21, 2024). Tidal range data are provided by University of Hawaii Sea Level Center (https://uhslc.soest.hawaii.edu/, last access: November 21, 2024). Sea surface temperature data are provided by NASA (https://oceandata.sci.gsfc.nasa.gov/cgi/getfile/AQUA_MODIS.20200101_20201231.L3m.YR.SST.sst.4km.nc, last access: November 21, 2024). Sea surface salinity data were obtained from the HYCOM consortium (https://developers.google.com/earth-engine/datasets/catalog/HYCOM_sea_temp_salinity, last access: November 21, 2024). Night lights data were obtained from the Earth Observation Group (https://eogdata.mines.edu/products/vnl/, last access: November 21, 2024). The global mangrove soil carbon for year 2020 version 4.0 database are provided by Earth and Environmental Sciences (https://dataverse.harvard.edu/dataset.xhtml?persistentId=doi:10.7910/DVN/OCYUIT, last access: November 21, 2024), and the global mangrove soil carbon data set at 30 m resolution for year 2020 (0–100 cm) version v1.2 is available at Zenodo (https://zenodo.org/records/7729492, last access: November 21, 2024).

ACKNOWLEDGMENTS

This research was funded by the National Key R&D Program of China grant (no. 2022YFF0803100), the National Natural Science Foundation of China (no.72394404 and 41701205), the National Key R&D Program of China (no. 2022YFC3105405), the Xiamen Natural Science Foundation grant (no. 3502Z20227011), the Fundamental Research Funds for the Central Universities (no. 20720240093), and the Internal Program of State Key Laboratory of Marine Environmental Science (no. MELRI2205). Thank you to Michael and Mathilda Cochran for endowing the Cochran Family Professorship in Earth and Environmental Sciences at Tulane University, which supported D.A.F. and Z.Z. Thanks also go to Dong Jinwei, Wang Wenqing, and Zhang Yamian for their valuable insights and suggestions on refining the article's structure and providing detailed knowledge on mangrove restoration.

AUTHOR CONTRIBUTIONS

Y.J., Z.Z., Yangfan Li, and Yi Li conceived the original idea and designed the overall study. Y.J. developed the model, performed the study, and interpreted the results, with key inputs from Z.Z., D.A.F., Yi Li, and Yangfan Li. Y.J., Z.Z., and Yi Li wrote the main manuscript, with important contributions from D.A.F. and Yangfan Li. Q.Z. designed the visualization. All authors discussed the results and revised the manuscript.

DECLARATION OF INTERESTS

The authors declare no competing interests.

SUPPLEMENTAL INFORMATION

Supplemental information can be found online at https://doi.org/10.1016/j.oneear.2024.11.003.

Received: December 27, 2023
Revised: August 13, 2024
Accepted: November 8, 2024
Published: December 2, 2024

REFERENCES

1. Barbier, E.B., Hacker, S.D., Kennedy, C., Koch, E.W., Stier, A.C., and Silliman, B.R. (2011). The value of estuarine and coastal ecosystem services. Ecol. Monogr. *81*, 169–193. https://doi.org/10.1890/10-1510.1.
2. Ribeiro, R.d.A., Rovai, A.S., Twilley, R.R., and Castañeda-Moya, E. (2019). Spatial variability of mangrove primary productivity in the neotropics. Ecosphere *10*, e02841. https://doi.org/10.1002/ecs2.2841.
3. Macreadie, P.I., Costa, M.D.P., Atwood, T.B., Friess, D.A., Kelleway, J.J., Kennedy, H., Lovelock, C.E., Serrano, O., and Duarte, C.M. (2021). Blue carbon as a natural climate solution. Nat. Rev. Earth Environ. *2*, 826–839. https://doi.org/10.1038/s43017-021-00224-1.
4. Goldberg, L., Lagomasino, D., Thomas, N., and Fatoyinbo, T. (2020). Global declines in human-driven mangrove loss. Global Change Biol. *26*, 5844–5855. https://doi.org/10.1111/gcb.15275.
5. Friess, D.A., Rogers, K., Lovelock, C.E., Krauss, K.W., Hamilton, S.E., Lee, S.Y., Lucas, R., Primavera, J., Rajkaran, A., and Shi, S. (2019). The state of the world's mangrove forests: past, present, and future. Annu. Rev. Environ. Resour. *44*, 89–115. https://doi.org/10.1146/annurev-environ-101718-033302.
6. Hamilton, S.E., and Friess, D.A. (2018). Global carbon stocks and potential emissions due to mangrove deforestation from 2000 to 2012. Nat. Clim. Change *8*, 240–244. https://doi.org/10.1038/s41558-018-0090-4.
7. Pendleton, L., Donato, D.C., Murray, B.C., Crooks, S., Jenkins, W.A., Sifleet, S., Craft, C., Fourqurean, J.W., Kauffman, J.B., Marbà, N., et al. (2012). Estimating global "blue carbon" emissions from conversion and degradation of vegetated coastal ecosystems. PLoS One *7*, e43542. https://doi.org/10.1371/journal.pone.0043542.
8. Arkema, K.K., Delevaux, J.M.S., Silver, J.M., Winder, S.G., Schile-Beers, L.M., Bood, N., Crooks, S., Douthwaite, K., Durham, C., Hawthorne, P.L., et al. (2023). Evidence-based target setting informs blue carbon strategies for nationally determined contributions. Nat. Ecol. Evol. *7*, 1045–1059. https://doi.org/10.1038/s41559-023-02081-1.
9. Thiam, E. (2023). The Mangrove Breakthrough (Global Mangrove Alliance). https://www.mangrovealliance.org/news/the-mangrove-breakthrough/.
10. Worthington, T., and Spalding, M. (2018). Mangrove Restoration Potential: A Global Map Highlighting a Critical Opportunity. Nat. Conserv. https://doi.org/10.17863/CAM.39153.
11. Arifanti, V.B., Kauffman, J.B., Novita, N., Subarno, Ilman, M., Ilman, M., and Tosiani, A. (2022). Contributions of mangrove conservation and restoration to climate change mitigation in Indonesia. Global Change Biol. *28*, 4523–4538. https://doi.org/10.1111/gcb.16216.
12. Sasmito, S.D., Basyuni, M., Kridalaksana, A., Saragi-Sasmito, M.F., Lovelock, C.E., and Murdiyarso, D. (2023). Challenges and opportunities for achieving Sustainable Development Goals through restoration of Indonesia's mangroves. Nat. Ecol. Evol. *7*, 62–70. https://doi.org/10.1038/s41559-022-01926-5.
13. Kodikara, K.A.S., Mukherjee, N., Jayatissa, L.P., Dahdouh-Guebas, F., and Koedam, N. (2017). Have mangrove restoration projects worked? An in-depth study in Sri Lanka. Restor. Ecol. *25*, 705–716. https://doi.org/10.1111/rec.12492.
14. Rodríguez-Rodríguez, J.A., Mancera-Pineda, J.E., and Tavera, H. (2021). Mangrove restoration in Colombia: Trends and lessons learned. For. Ecol. Manag. *496*, 119414. https://doi.org/10.1016/j.foreco.2021.119414.
15. Song, S., Ding, Y., Li, W., Meng, Y., Zhou, J., Gou, R., Zhang, C., Ye, S., Saintilan, N., Krauss, K.W., et al. (2023). Mangrove reforestation provides greater blue carbon benefit than afforestation for mitigating global climate change. Nat. Commun. *14*, 756. https://doi.org/10.1038/s41467-023-36477-1.
16. Wodehouse, D.C., and Rayment, M.B. (2019). Mangrove area and propagule number planting targets produce sub-optimal rehabilitation and afforestation outcomes. Estuar. Coast Shelf Sci. *222*, 91–102. https://doi.org/10.1016/j.ecss.2019.04.003.
17. Hamilton, S. (2013). Assessing the Role of Commercial Aquaculture in Displacing Mangrove Forest. Bull. Mar. Sci. *89*, 585–601. https://doi.org/10.5343/bms.2012.1069.
18. Ren, C., Wang, Z., Zhang, Y., Zhang, B., Chen, L., Xi, Y., Xiao, X., Doughty, R.B., Liu, M., Jia, M., et al. (2019). Rapid expansion of coastal aquaculture ponds in China from Landsat observations during 1984–2016. Int. J. Appl. Earth Obs. Geoinf. *82*, 101902. https://doi.org/10.1016/j.jag.2019.101902.
19. Richards, D.R., and Friess, D.A. (2016). Rates and drivers of mangrove deforestation in Southeast Asia, 2000–2012. Proc. Natl. Acad. Sci. USA *113*, 344–349. https://doi.org/10.1073/pnas.1510272113.
20. Zhang, Y., Zhang, L., Kang, Y., Li, Y., Chen, Z., Li, R., Tian, C., Wang, W., and Wang, M. (2022). Biotic homogenization increases with human intervention: implications for mangrove wetland restoration. Ecography *2022*, e05835. https://doi.org/10.1111/ecog.05835.
21. Sakai, Y., Kouyama, T., Kakinuma, K.i., Sakaguchi, Y., Yuasa, N., Thongkao, S., Boonming, S., Chantrapromma, K., and Kato, S. (2023). Recovery of mangrove ecosystem carbon stocks through reforestation at abandoned shrimp pond in southeast thailand. Ecosyst. Health. Sustain *9*, 0018. https://doi.org/10.34133/ehs.0018.
22. Bunting, P., Rosenqvist, A., Hilarides, L., Lucas, R.M., Thomas, N., Tadono, T., Worthington, T.A., Spalding, M., Murray, N.J., and Rebelo, L.-M. (2022). Global mangrove extent change 1996–2020: global mangrove watch version 3.0. Rem. Sens. *14*, 3657. https://doi.org/10.3390/rs14153657.
23. Baltezar, P., Murillo-Sandoval, P.J., Cavanaugh, K.C., Doughty, C., Lagomasino, D., Tieng, T., Simard, M., and Fatoyinbo, T. (2023). A regional map of mangrove extent for Myanmar, Thailand, and Cambodia shows losses of 44% by 1996. Front. Mar. Sci. *10*, 1127720. https://doi.org/10.3389/fmars.2023.1127720.

24. Primavera, J.H. (2000). Development and conservation of Philippine mangroves: institutional issues. Ecol. Econ. *35*, 91–106. https://doi.org/10.1016/S0921-8009(00)00170-1.

25. Ilman, M., Dargusch, P., and Dart, P.; Onrizal (2016). A historical analysis of the drivers of loss and degradation of Indonesia's mangroves. Land Use Pol. *54*, 448–459. https://doi.org/10.1016/j.landusepol.2016.03.010.

26. Luo, J., Sun, Z., Lu, L., Xiong, Z., Cui, L., and Mao, Z. (2022). Rapid expansion of coastal aquaculture ponds in Southeast Asia: patterns, drivers and impacts. J. Environ. Manag. *315*, 115100. https://doi.org/10.1016/j.jenvman.2022.115100.

27. Akber, M.A., Aziz, A.A., and Lovelock, C. (2020). Major drivers of coastal aquaculture expansion in Southeast Asia. Ocean Coast Manag. *198*, 105364. https://doi.org/10.1016/j.ocecoaman.2020.105364.

28. Sidik, F., Supriyanto, B., Krisnawati, H., and Muttaqin, M.Z. (2018). Mangrove conservation for climate change mitigation in Indonesia. WIREs Clim. Change *9*, e529. https://doi.org/10.1002/wcc.529.

29. Spalding, M.D., and Leal, M. (2021). The State of the World's Mangroves 2021 (Global Mangrove Alliance).

30. Zhang, Z., Li, J., Li, Y., Liu, W., Chen, Y., Zhang, Y., and Li, Y. (2021). Spatially discontinuous relationships between salt marsh invasion and mangrove forest fragmentation. For. Ecol. Manage. *499*, 119611. https://doi.org/10.1016/j.foreco.2021.119611.

31. Haddad, N.M., Brudvig, L.A., Clobert, J., Davies, K.F., Gonzalez, A., Holt, R.D., Lovejoy, T.E., Sexton, J.O., Austin, M.P., Collins, C.D., et al. (2015). Habitat fragmentation and its lasting impact on earth's ecosystems. Sci. Adv. *1*, e1500052. https://doi.org/10.1126/sciadv.1500052.

32. Nagelkerken, I., Blaber, S.J.M., Bouillon, S., Green, P., Haywood, M., Kirton, L.G., Meynecke, J.-O., Pawlik, J., Penrose, H.M., Sasekumar, A., and Somerfield, P. (2008). The habitat function of mangroves for terrestrial and marine fauna: a review. Aquat. Bot. *89*, 155–185. https://doi.org/10.1016/j.aquabot.2007.12.007.

33. Krauss, K.W., Lovelock, C.E., McKee, K.L., López-Hoffman, L., Ewe, S.M., and Sousa, W.P. (2008). Environmental drivers in mangrove establishment and early development: a review. Aquat. Bot. *89*, 105–127. https://doi.org/10.1016/j.aquabot.2007.12.014.

34. Van Loon, A.F., Te Brake, B., Van Huijgevoort, M.H.J., and Dijksma, R. (2016). Hydrological classification, a practical tool for mangrove restoration. PLoS One *11*, e0150302. https://doi.org/10.1371/journal.pone.0150302.

35. Cannon, D., Kibler, K., Donnelly, M., McClenachan, G., Walters, L., Roddenberry, A., and Phagan, J. (2020). Hydrodynamic habitat thresholds for mangrove vegetation on the shorelines of a microtidal estuarine lagoon. Ecol. Eng. *158*, 106070. https://doi.org/10.1016/j.ecoleng.2020.106070.

36. Lewis, R.R. (2005). Ecological engineering for successful management and restoration of mangrove forests. Ecol. Eng. *24*, 403–418. https://doi.org/10.1016/j.ecoleng.2004.10.003.

37. Kamali, B., and Hashim, R. (2011). Mangrove restoration without planting. Ecol. Eng. *37*, 387–391. https://doi.org/10.1016/j.ecoleng.2010.11.025.

38. Zhu, X., Hou, Y., Weng, Q., and Chen, L. (2019). Integrating UAV optical imagery and LiDAR data for assessing the spatial relationship between mangrove and inundation across a subtropical estuarine wetland. ISPRS J. Photogrammetry Remote Sens. *149*, 146–156. https://doi.org/10.1016/j.isprsjprs.2019.01.021.

39. Langston, A.K., Alexander, C.R., Alber, M., and Kirwan, M.L. (2021). Beyond 2100: Elevation capital disguises salt marsh vulnerability to sea-level rise in Georgia, USA. Estuar. Coast Shelf Sci. *249*, 107093. https://doi.org/10.1016/j.ecss.2020.107093.

40. Harris, N.L., Gibbs, D.A., Baccini, A., Birdsey, R.A., de Bruin, S., Farina, M., Fatoyinbo, L., Hansen, M.C., Herold, M., Houghton, R.A., et al. (2021). Global maps of twenty-first century forest carbon fluxes. Nat. Clim. Change *11*, 234–240. https://doi.org/10.1038/s41558-020-00976-6.

41. Ricke, K., Drouet, L., Caldeira, K., and Tavoni, M. (2018). Country-level social cost of carbon. Nat. Clim. Change *8*, 895–900. https://doi.org/10.1038/s41558-018-0282-y.

42. Bayraktarov, E., Saunders, M.I., Abdullah, S., Mills, M., Beher, J., Possingham, H.P., Mumby, P.J., and Lovelock, C.E. (2016). The cost and feasibility of marine coastal restoration. Ecol. Appl. *26*, 1055–1074. https://doi.org/10.1890/15-1077.

43. Su, J., Friess, D.A., and Gasparatos, A. (2021). A meta-analysis of the ecological and economic outcomes of mangrove restoration. Nat. Commun. *12*, 5050. https://doi.org/10.1038/s41467-021-25349-1.

44. Carbon exchange CIX completes 250,000 tonne carbon credit auction (2022). Reuters. https://www.reuters.com/business/environment/carbon-exchange-cix-completes-250000-tonne-carbon-credit-auction-2022-11-04/.

45. Bertram, C., Quaas, M., Reusch, T.B.H., Vafeidis, A.T., Wolff, C., and Rickels, W. (2021). The blue carbon wealth of nations. Nat. Clim. Change *11*, 704–709. https://doi.org/10.1038/s41558-021-01089-4.

46. Sidik, F., Lawrence, A., Wagey, T., Zamzani, F., and Lovelock, C.E. (2023). Blue carbon: a new paradigm of mangrove conservation and management in Indonesia. Mar. Pol. *147*, 105388. https://doi.org/10.1016/j.marpol.2022.105388.

47. Zeng, Y., Friess, D.A., Sarira, T.V., Siman, K., and Koh, L.P. (2021). Global potential and limits of mangrove blue carbon for climate change mitigation. Curr. Biol. *31*, 1737–1743.e3. https://doi.org/10.1016/j.cub.2021.01.070.

48. Friess, D.A., Gatt, Y.M., Ahmad, R., Brown, B.M., Sidik, F., and Wodehouse, D. (2022). Achieving ambitious mangrove restoration targets will need a transdisciplinary and evidence-informed approach. One Earth *5*, 456–460. https://doi.org/10.1016/j.oneear.2022.04.013.

49. Lovelock, C.E., and Brown, B.M. (2019). Land tenure considerations are key to successful mangrove restoration. Nat. Ecol. Evol. *3*, 1135. https://doi.org/10.1038/s41559-019-0942-y.

50. Sanderman, J., Hengl, T., Fiske, G., Solvik, K., Adame, M.F., Benson, L., Bukoski, J.J., Carnell, P., Cifuentes-Jara, M., Donato, D., et al. (2018). A global map of mangrove forest soil carbon at 30 m spatial resolution. Environ. Res. Lett. *13*, 055002. https://doi.org/10.1088/1748-9326/aabe1c.

51. Atwood, T.B., Connolly, R.M., Almahasheer, H., Carnell, P.E., Duarte, C.M., Ewers Lewis, C.J., Irigoien, X., Kelleway, J.J., Lavery, P.S., Macreadie, P.I., et al. (2017). Global patterns in mangrove soil carbon stocks and losses. Nat. Clim. Change *7*, 523–528. https://doi.org/10.1038/nclimate3326.

52. Bryan-Brown, D.N., Connolly, R.M., Richards, D.R., Adame, F., Friess, D.A., and Brown, C.J. (2020). Global trends in mangrove forest fragmentation. Sci. Rep. *10*, 7117. https://doi.org/10.1038/s41598-020-63880-1.

53. Herbeck, L.S., Krumme, U., Andersen, T.J., and Jennerjahn, T.C. (2020). Decadal trends in mangrove and pond aquaculture cover on Hainan (China) since 1966: mangrove loss, fragmentation and associated biogeochemical changes. Estuar. Coast Shelf Sci. *233*, 106531. https://doi.org/10.1016/j.ecss.2019.106531.

54. Duan, Y., Li, X., Zhang, L., Chen, D., Liu, S., and Ji, H. (2020). Mapping national-scale aquaculture ponds based on the Google Earth Engine in the Chinese coastal zone. Aquaculture *520*, 734666. https://doi.org/10.1016/j.aquaculture.2019.734666.

55. NASA, L.P.D. (2013). NASA Shuttle Radar Topography Mission (SRTM) Version 3.0 (SRTM Plus) Product Release (National Aeronautics and Space Administration).

56. Foga, S., Scaramuzza, P.L., Guo, S., Zhu, Z., Dilley, R.D., Beckmann, T., Schmidt, G.L., Dwyer, J.L., Joseph Hughes, M., and Laue, B. (2017). Cloud detection algorithm comparison and validation for operational Landsat data products. Remote Sens. Environ. *194*, 379–390. https://doi.org/10.1016/j.rse.2017.03.026.

57. Murray, N.J., Phinn, S.R., DeWitt, M., Ferrari, R., Johnston, R., Lyons, M.B., Clinton, N., Thau, D., and Fuller, R.A. (2019). The global distribution and trajectory of tidal flats. Nature *565*, 222–225. https://doi.org/10.1038/s41586-018-0805-8.

58. Otsu, N. (1979). A Threshold Selection Method from Gray-Level Histograms. IEEE Trans. Syst. Man Cybern. *9*, 62–66. https://doi.org/10.1109/TSMC.1979.4310076.

59. Jiang, Y., Li, J., Zhang, Z., and Li, Y. (2024). Dynamics of coastal land-based aquaculture pond in China and Southeast Asia from 1990 to 2020. Int. J. Appl. Earth Obs. Geoinf. *127*, 103654. https://doi.org/10.1016/j.jag.2024.103654.

60. Bunting, P., Rosenqvist, A., Lucas, R.M., Rebelo, L.-M., Hilarides, L., Thomas, N., Hardy, A., Itoh, T., Shimada, M., and Finlayson, C.M. (2018). The global mangrove watch—a new 2010 global baseline of mangrove extent. Rem. Sens. *10*, 1669. https://doi.org/10.3390/rs10101669.

61. Long, J.B., and Giri, C. (2011). Mapping the Philippines' mangrove forests using Landsat imagery. Sensors *11*, 2972–2981. https://doi.org/10.3390/s110302972.

62. Zanaga, D., Van, D.K., Ruben, Keersmaecker, D., Wanda, Souverijns, Niels, B., Carsten, Q., Ralf, W., Jan, G., et al. (2021). ESA WorldCover 10 m 2020 v100. Zenodo. https://doi.org/10.5281/ZENODO.5571936 Version v100. .

63. Kamali, B., and Hashim, R. (2011). Mangrove restoration without planting. Ecol. Eng. *37*, 387–391. https://doi.org/10.1016/j.ecoleng.2010.11.025.

64. Saintilan, N., Khan, N.S., Ashe, E., Kelleway, J.J., Rogers, K., Woodroffe, C.D., and Horton, B.P. (2020). Thresholds of mangrove survival under rapid sea level rise. Science *368*, 1118–1121. https://doi.org/10.1126/science.aba2656.

65. Leung, J.Y. (2015). Habitat heterogeneity affects ecological functions of macrobenthic communities in a mangrove: Implication for the impact of restoration and afforestation. Glob. Ecol. Conserv. *4*, 423–433. https://doi.org/10.1016/j.gecco.2015.08.005.

66. Peters, J.R., Yeager, L.A., and Layman, C.A. (2015). Comparison of fish assemblages in restored and natural mangrove habitats along an urban shoreline. Bull. Mar. Sci. *91*, 125–139. https://doi.org/10.5343/bms.2014.1063.

67. Alongi, D.M. (2015). The impact of climate change on mangrove forests. Curr. Clim. Change Rep. *1*, 30–39. https://doi.org/10.1007/s40641-015-0002-x.

68. Cummings, J.A., and Smedstad, O.M. (2013). Variational Data Assimilation for the Global Ocean. In Data Assimilation for Atmospheric, Oceanic and Hydrologic Applications, *II*, S.K. Park and L. Xu, eds. *(Springer), pp. 303–343. https://doi.org/10.1007/978-3-642-35088-7_13.*

69. Blanco-Sacristán, J., Johansen, K., Duarte, C.M., Daffonchio, D., Hoteit, I., and McCabe, M.F. (2022). Mangrove distribution and afforestation potential in the Red Sea. Sci. Total Environ. *843*, 157098. https://doi.org/10.1016/j.scitotenv.2022.157098.

70. Franklin, J., and Miller, J.A. (2009). Mapping Species Distributions: Spatial Inference and Prediction, *338* (Cambridge University Press).

71. Phillips, S.J., Dudík, M., and Schapire, R.E. (2004). A maximum entropy approach to species distribution modeling. In Proceedings of the 21st International Conference on Machine learning (ACM), p. 83. https://doi.org/10.1145/1015330.1015412.

72. Donato, D.C., Kauffman, J.B., Murdiyarso, D., Kurnianto, S., Stidham, M., and Kanninen, M. (2011). Mangroves among the most carbon-rich forests in the tropics. Nat. Geosci. *4*, 293–297. https://doi.org/10.1038/ngeo1123.

73. Breithaupt, J.L., Smoak, J.M., Smith, T.J., III, Sanders, C.J., and Hoare, A. (2012). Organic carbon burial rates in mangrove sediments: Strengthening the global budget. Global Biogeochem. Cycles *26*, GB3011. https://doi.org/10.1029/2012GB004375.

74. Hutchison, J., Manica, A., Swetnam, R., Balmford, A., and Spalding, M. (2014). Predicting global patterns in mangrove forest biomass. Conserv. Lett. *7*, 233–240. https://doi.org/10.1111/conl.12060.

75. Saenger, P., and Snedaker, S.C. (1993). Pantropical trends in mangrove above-ground biomass and annual litterfall. Oecologia *96*, 293–299. https://doi.org/10.1007/BF00317496.

76. Komiyama, A., Jintana, V., Sangtiean, T., and Kato, S. (2002). A common allometric equation for predicting stem weight of mangroves growing in secondary forests. Ecol. Res. *17*, 415–418. https://doi.org/10.1046/j.1440-1703.2002.00500.x.

77. Komiyama, A., Ong, J.E., and Poungparn, S. (2008). Allometry, biomass, and productivity of mangrove forests: a review. Aquat. Bot. *89*, 128–137. https://doi.org/10.1016/j.aquabot.2007.12.006.

78. Kauffman, J.B., and Donato, D.C. (2012). Protocols for the Measurement, Monitoring and Reporting of Structure, Biomass and Carbon Stocks in Mangrove Forests (Indonesia: Center for International Forestry Research, Bogor).

79. Hamilton, S.E., and Lovette, J. (2015). Ecuador's mangrove forest carbon stocks: a spatiotemporal analysis of living carbon holdings and their depletion since the advent of commercial aquaculture. PLoS One *10*, e0118880. https://doi.org/10.1371/journal.pone.0118880.

80. Hiraishi, T., Krug, T., Tanabe, K., Srivastava, N., Jamsranjav, B., Fukuda, M., and Troxler, T. (2014). 2013 Supplement to the 2006 IPCC Guidelines for National Greenhouse Gas Inventories: Wetlands (IPCC).

81. Maxwell, T.L., Hengl, T., Parente, L.L., Minarik, R., Worthington, T.A., Bunting, P., Smart, L.S., Spalding, M.D., and Landis, E. (2023). Global mangrove soil organic carbon stocks dataset at 30 m resolution for the year 2020 based on spatiotemporal predictive machine learning. Data Brief *50*, 109621. https://doi.org/10.1016/j.dib.2023.109621.

82. Sasmito, S.D., Taillardat, P., Clendenning, J.N., Cameron, C., Friess, D.A., Murdiyarso, D., and Hutley, L.B. (2019). Effect of land-use and land-cover change on mangrove blue carbon: a systematic review. Global Change Biol. *25*, 4291–4302. https://doi.org/10.1111/gcb.14774.

83. Adame, M.F., Connolly, R.M., Turschwell, M.P., Lovelock, C.E., Fatoyinbo, T., Lagomasino, D., Goldberg, L.A., Holdorf, J., Friess, D.A., Sasmito, S.D., et al. (2021). Future carbon emissions from global mangrove forest loss. Global Change Biol. *27*, 2856–2866. https://doi.org/10.1111/gcb.15571.

84. Hamilton, S.E., and Casey, D. (2016). Creation of a high spatio-temporal resolution global database of continuous mangrove forest cover for the 21st century (CGMFC-21). Global Ecol. Biogeogr. *25*, 729–738. https://doi.org/10.1111/geb.12449.

85. Sillanpää, M., Vantellingen, J., and Friess, D.A. (2017). Vegetation regeneration in a sustainably harvested mangrove forest in West Papua, Indonesia. For. Ecol. Manag. *390*, 137–146. https://doi.org/10.1016/j.foreco.2017.01.022.

86. Bourgeois, C.F., MacKenzie, R.A., Sharma, S., Bhomia, R.K., Johnson, N.G., Rovai, A.S., Worthington, T.A., Krauss, K.W., Analuddin, K., Bukoski, J.J., et al. (2024). Four decades of data indicate that planted mangroves stored up to 75% of the carbon stocks found in intact mature stands. Sci. Adv. *10*, eadk5430. https://doi.org/10.1126/sciadv.adk5430.

87. Breithaupt, J.L., and Steinmuller, H.E. (2022). Refining the Global Estimate of Mangrove Carbon Burial Rates Using Sedimentary and Geomorphic Settings. Geophys. Res. Lett. *49*, e2022GL100177. https://doi.org/10.1029/2022GL100177.

88. Hu, T., Zhang, Y., Su, Y., Zheng, Y., Lin, G., and Guo, Q. (2020). Mapping the Global Mangrove Forest Aboveground Biomass Using Multisource Remote Sensing Data. Rem. Sens. *12*, 1690. https://doi.org/10.3390/rs12101690.

89. Pham, V.H., Luu, V.D., Nguyen, T.T., and Koji, O. (2017). Will restored mangrove forests enhance sediment organic carbon and ecosystem carbon storage? Reg. Stud. Mar. Sci. *14*, 43–52. https://doi.org/10.1016/j.rsma.2017.05.003.

90. Xiong, Y., Liao, B., and Wang, F. (2018). Mangrove vegetation enhances soil carbon storage primarily through *in situ* inputs rather than increasing allochthonous sediments. Mar. Pollut. Bull. *131*, 378–385. https://doi.org/10.1016/j.marpolbul.2018.04.043.

91. Sasmito, S.D., Kuzyakov, Y., Lubis, A.A., Murdiyarso, D., Hutley, L.B., Bachri, S., Friess, D.A., Martius, C., and Borchard, N. (2020). Organic carbon burial and sources in soils of coastal mudflat and mangrove ecosystems. Catena *187*, 104414. https://doi.org/10.1016/j.catena.2019.104414.

92. Bansal, R., Kiku, D., and Ochoa, M. (2016). Price of Long-Run Temperature Shifts in Capital Markets. Natl. Bur. Econ. Res, 1–57. https://doi.org/10.3386/w22529.

93. Anthoff, D., and Tol, R.S.J. (2013). The uncertainty about the social cost of carbon: a decomposition analysis using fund. Clim. Change *117*, 515–530. https://doi.org/10.1007/s10584-013-0706-7.

94. Moore, F.C., and Diaz, D.B. (2015). Temperature impacts on economic growth warrant stringent mitigation policy. Nat. Clim. Change *5*, 127–131. https://doi.org/10.1038/nclimate2481.

95. Nordhaus, W. (2014). Estimates of the social cost of carbon: concepts and results from the DICE-2013R model and alternative approaches. J. Assoc. Environ. Resour. Econ. *1*, 273–312. https://doi.org/10.1086/676035.

96. Friess, D.A. (2023). The potential for mangrove and seagrass blue carbon in Small Island States. Curr. Opin. Environ. Sustain. *64*, 101324. https://doi.org/10.1016/j.cosust.2023.101324.